

Effect of Er substituting sites on upconversion luminescence of Er³⁺-doped BaTiO₃ films

CHEN Lei, WEI Xian-hua, FU Xu

State Key Laboratory Cultivation Base for Nonmetal Composites and Functional Materials,
Southwest University of Science and Technology, Mianyang 621010, China

Received 22 June 2011; accepted 15 February 2012

Abstract: Erbium-doped BaTiO₃ films on LaNiO₃/Si substrates were fabricated by sol–gel method. The crystalline structure, morphologies and upconversion (UC) luminescence properties of films were respectively investigated by X-ray diffraction (XRD), atomic force microscopy (AFM) and photoluminescence (PL). The results indicate that both of the microstructure and luminescence are found to be dependent on Er³⁺ substituting sites. The samples with A-site substitution have smaller lattice constants, larger grains and smoother surface than those with B-site substitution. The photoluminescence spectra show that both of the samples have two stronger green emission bands centered at 528 and 548 nm and a weak red emission band centered at 673 nm, which correspond to the relaxation of Er³⁺ from ²H_{11/2}, ⁴S_{3/2}, and ⁴F_{9/2} levels to the ground level ⁴I_{15/2}, respectively. Compared with B-site doped films, A-site doped films have a stronger integrated intensity of green emissions and a weaker relative intensity of red emissions. The differences could be explained by the crystalline quality and cross relaxation (CR) process.

Key words: Er³⁺ doping; BaTiO₃ thin films; upconversion photoluminescence; sol–gel method

1 Introduction

Ferroelectric thin films for integrated optics have received much attention due to their potential applications in second-harmonic generation, high speed modulators and gain devices. Barium titanate (BaTiO₃) is a good thin film integrated optic host because of its superior electronic and electro-optic properties, compared with other ferroelectric materials. For example, it has high electro-optic coefficient (820 pm/V at 632.8 nm, higher than 30.8 pm/V of LiNbO₃) [1,2], low half-wave voltage (310 V at 632.8 nm, lower than 2940 V of LiNbO₃) [3], low-loss waveguides ($\leq(4 \pm 2)$ dB/cm) and high solid solubility of rare earth ions [3,4]. Er³⁺ as an active ion can meet the request used for upconversion (UC) phosphors, planar waveguide and structural probe [5–8]. A lot of work about UC properties has been reported on Er³⁺-doped BaTiO₃ films [3,4,6,9]. It is noted that both of the valence state and the radius of Er³⁺ ion are intermediate between those of Ba²⁺ ion and Ti⁴⁺ ion. As a result, Er³⁺ can occupy either A- or B-site depending on Ba/Ti mole ratio [8,10–12]. It is

well-known that crystal field caused by structure symmetry of the host materials would result in different perturbation in terms of Er³⁺ inner shell transitions. Therefore, UC photoluminescence should be dependent on the excited-state dynamics of the Er³⁺ ions and their interactions with the host matrix [8,13]. Unfortunately, little attention has been paid to the effect of Er substituting sites on UC photoluminescence properties. Recently, the UC properties of Er³⁺-doped BaTiO₃ ceramics were correlated with doping concentrations, phase structure and doping sites [8,14]. Furthermore, the emission from substituted Er³⁺ ions might be considered structural probe for the ferroelectrics. In this work, the influence of substitution site of Er³⁺-doped BaTiO₃ films on their photoluminescence properties is investigated. Er³⁺-doped BaTiO₃ thin films with different doping sites are deposited on LaNiO₃/Si substrate by sol–gel method.

2 Experimental

Er³⁺-doped BaTiO₃ films were prepared by a modified sol–gel method. According to the charge compensation mechanism, the charge neutrality should

be maintained through the vacancy formation of barium and oxygen for those samples with A-site and B-site substitution of Er^{3+} , respectively. So, the formulas should be respectively $\text{Ba}_{1-3x/2}\text{Er}_x\text{TiO}_3$ and $\text{BaTi}_{1-x}\text{Er}_x\text{O}_{3-\delta}$. Here the value of x is 0.03, which has been proved to show a strong UC photoluminescence [15]. The whole process of preparing the solution is described in Fig. 1. Barium acetate $[\text{Ba}(\text{Ac})_2]$, titanium butoxide $[\text{Ti}(\text{C}_4\text{H}_9\text{O})_4, \text{Ti}(\text{O}-\text{Bu})_4]$, erbium acetate $[\text{Er}(\text{Ac})_3]$ were used as starting materials; acetyl acetone $[\text{AcAc}, \text{C}_5\text{H}_8\text{O}_2]$, acetic acid (HAc) were used as solvents of $\text{Ti}(\text{O}-\text{Bu})_4$ and $\text{Ba}(\text{Ac})_2$ respectively. 2-methoxyethanol was used as solvent for the whole solution. The concentration of the solutions was adjusted to 0.4 mol/L through the addition of ethylene glycol. A light brown-yellow and transparent precursor appeared in the final sol. The LaNiO_3/Si substrates were first cleaned with acetone and ethanol, later rinsed with deionized water in a sonic bath. Spin-coating of the solutions was performed at 500 r/min for 18 s and 4000 r/min for 30 s on LaNiO_3/Si substrates. After coating, each layer was dried at 200 °C for 10 min and then baked at 400 °C for 10 min in air. This process was repeated until the desired thickness of about 500 nm was attained. Finally, the samples were annealed in oxygen at 750 °C for 2 h.

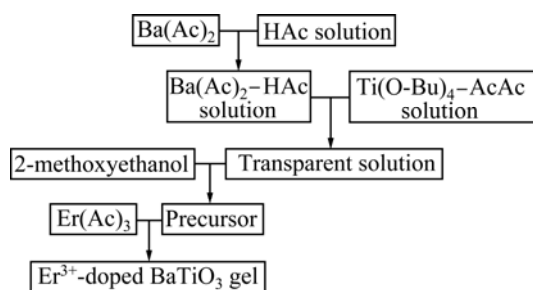


Fig. 1 Process of preparing Er^{3+} -doped BaTiO_3 solutions

Thermogravimetric analysis (TGA) and differential thermal analysis (DTA) of dried gel were carried out on METTLER TOLEDO (TGA/SDTA 851^o) from the room temperature to 800 °C in an oxygen flux with a heating rate of 10 °C/min. The crystal structure of the thin films was analyzed by an X-ray diffractometer (XRD, Philips X'pert MPD Pro) utilizing $\text{Cu K}\alpha$ (wavelength: $\lambda=1.5406 \text{ \AA}$) radiation. Atomic force microscope (AFM, Seiko SPI 3800) was used to investigate the grain size and surface roughness. The photoluminescence spectra were characterized by the use of Edinburgh FLSP920 spectrofluorophotometer at room temperature. The excitation light for UC luminescence was a 980 nm laser diode with a power of 500 mW. The excitation beams were applied directly onto the film surface and the signals were collected in the front of the films.

3 Results and discussion

3.1 DTA and TG

Figure 2 shows the TGA, DrTGA (derivative of TGA) and DTA results of BaTiO_3 dry gel. The first peak of DrTGA (the inset of Fig. 2) appears at about 100 °C, indicating the loss of water in dry gel. Significant mass losses of about 1.6 mg and 2 mg are observed in temperature range of 100–300 °C and 300–450 °C, respectively. These may be due to the decomposition and combustion process of the organic compounds, which are in agreement with the exothermic peaks in DTA curve. The two peaks at 600 °C and 700 °C corresponding to the mass loss of about 0.5 mg and 0.3 mg represent the complete decomposition of the organic compounds and the formation of crystallized BaTiO_3 , respectively. Therefore, the treatment temperatures of films are selected as 400 °C for the baking process and 750 °C for the final annealing process.

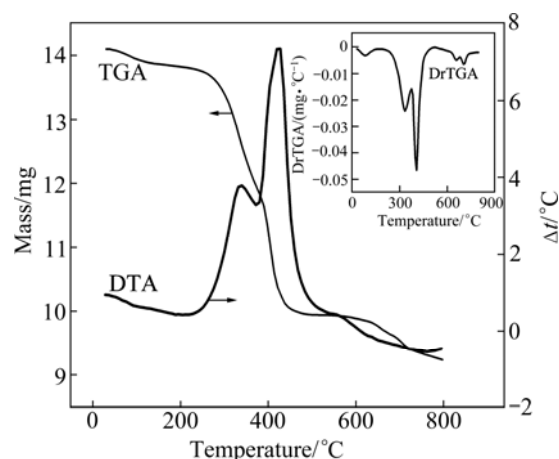


Fig. 2 Thermal analysis results of BaTiO_3

3.2 X-ray diffraction patterns and atomic force microscopy image

Figure 3(a) presents the XRD patterns of Er^{3+} -doped BaTiO_3 thin films annealed at 750 °C. Only the diffraction peaks from phase-pure crystalline BaTiO_3 is observed besides the existence of the information of the substrates in both cases. The result implies that Er^{3+} ions were doped efficiently into different sites of BaTiO_3 host. There are minor shifts of the diffraction peak (200) between the Er^{3+} -doped samples, as shown in Fig. 3(b), meaning that the lattices of the films could be slightly deformed because of the doping of impurity ions. In two cases, no obvious splitting of cubic (200) into tetragonal (200) and (002) reflections at about 45° can be observed. It remains difficult to assign the crystal structure of BaTiO_3 films to either cubic or tetragonal symmetry using conventional X-ray diffractometer due to line broadening [16]. Otherwise, it should be induced

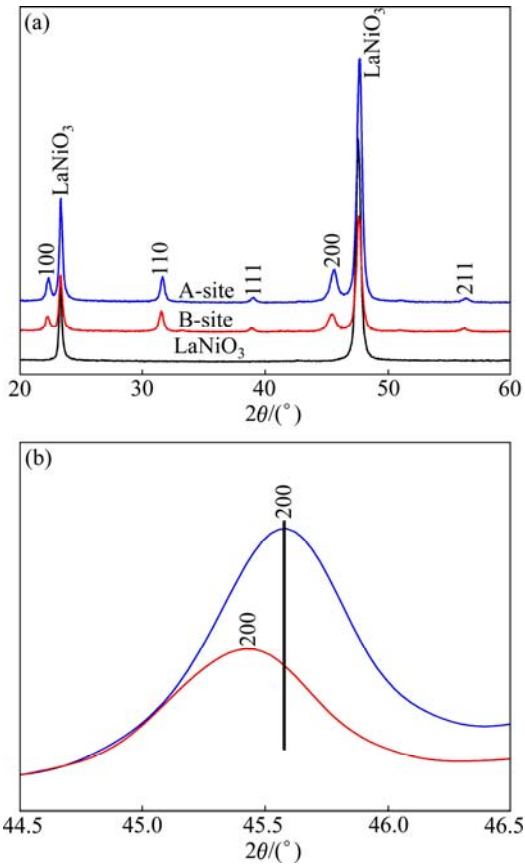


Fig. 3 XRD patterns of films doped with 3% Er^{3+} for A- and B-site BaTiO_3 substitution annealed at 750 °C (a) and enlarged (200) peak (b)

by the size effect. Here the BaTiO_3 lattice was regarded as cubic phase with the lattice parameter of 3.9820 Å for the undoped sample (JCPDS Card No.74—1956). The computed lattices are respectively 3.9745 Å and 3.9872 Å from the XRD results for the A-site and B-site doped films, indicating the contraction and expansion of the lattice [8,17].

Moreover, the FWHM of B-site substitution sample is larger than that of A-site substitution one, indicative of the smaller grains. It can be further proved by AFM analysis shown in Fig. 4. The films of A-site substitution have a well-crystallized and dense surface with the average grain size of about 60 nm and the RMS roughness of 4.0 nm. On the other hand, the samples of B-site substitution show the smaller grain size of about 40 nm and the larger RMS value of 8.4 nm (not shown here). The difference of the crystalline quality should be associated with the oxygen-deficient nonstoichiometry in B-site doped films.

3.3 UC photoluminescence

The PL spectra of BaTiO_3 films with different Er^{3+} ion site substitutions are measured under excitation of 980 nm, as shown in Fig. 5. The typical UC emission

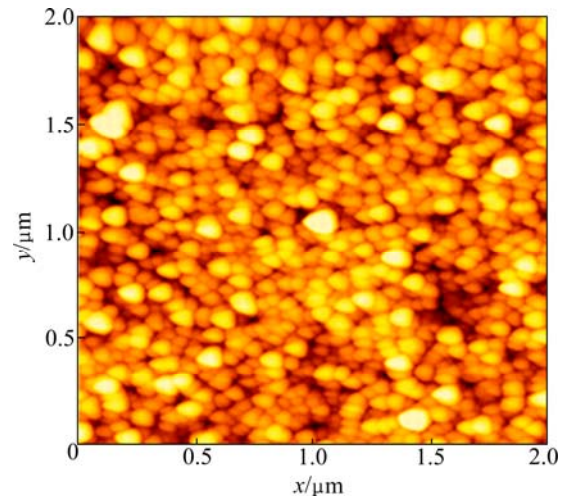


Fig. 4 AFM micrograph of 3% Er^{3+} -doped BaTiO_3 film with A-site

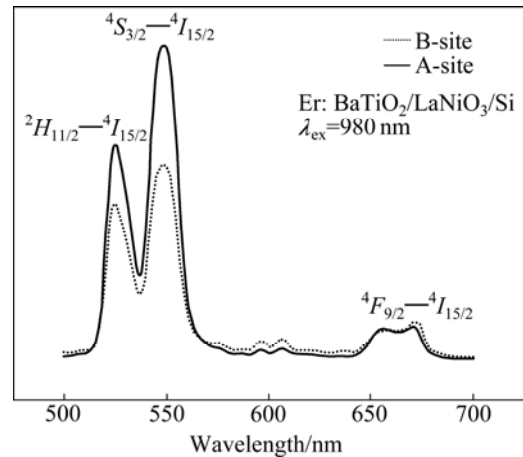


Fig. 5 Integrated intensity of BaTiO_3 doped with 3% Er^{3+} for A- and B-site substitutions

consists of two strong green bands located at 528 and 548 nm corresponding to ${}^2H_{11/2}/{}^4S_{3/2} \rightarrow {}^4I_{15/2}$ transitions, and a weak red emission band at 673 nm associated with ${}^4F_{9/2} \rightarrow {}^4I_{15/2}$ transition of the Er^{3+} ions, respectively. The intensity ratio of 528 and 548 nm (I_{548}/I_{528}) is about 1.35 for both of the cases, while the relative ratios of green and red (I_{548}/I_{673}) are respectively 9.25 and 4.83 for A-site substitution and B-site substitution. There is no obvious shift of the emission peaks. These results indicate that the crystal field surrounding the erbium ions can change the relative probability of the transitions from the excited state to the ${}^4I_{15/2}$ ground state. The UC luminescence mechanisms are mainly determined by the process of excited state absorption (ESA) and energy transfer (ET). As shown in Fig. 6, under the excitation of 980 nm, through ESA or ET process, Er^{3+} ion can populate the ${}^4F_{7/2}$ level. Subsequently, the Er^{3+} ion then relaxes nonradiatively to the ${}^2H_{11/2}$, ${}^4S_{3/2}$ and ${}^4F_{9/2}$ levels by multiphonon relaxation, from which the strong green ${}^2H_{11/2}/{}^4S_{3/2} \rightarrow {}^4I_{15/2}$ emissions and the weak red ${}^4F_{9/2} \rightarrow$

$^4I_{15/2}$ occur. The ESA approach only occurs during excitation, whereas the ET can happen both during and after the excitation. For the 673 nm red emission, due to the large energy gap between $^4S_{3/2}$ and $^4F_{9/2}$ levels, the nonradiative relaxation probability from the $^4S_{3/2}$ level to the $^4F_{9/2}$ level is quite low. Therefore, the intensity of the red emissions is weaker than that of green emissions [18].

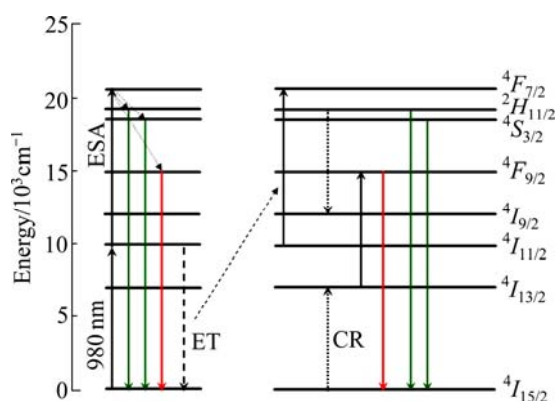


Fig. 6 Possible UC photoluminescence mechanisms of 3% Er^{3+} -doped BaTiO_3 films

The integrated intensity of A-site doped sample is much stronger than that of B-site doped BaTiO_3 film. It is mainly affected by the crystalline condition which A-site substitution has a better crystalline. But there is no difference between them in the value of I_{548}/I_{528} , which indicates that the ratio of I_{548} to I_{528} has no great importance in different substituting positions and crystalline conditions. As for the large difference of I_{548}/I_{673} , it could be understood by cross-relaxation (CR) shown in Fig. 6. As we known, subband gap defect levels could participate in the relaxation process and change the probability of radiative recombination [8, 19, 20]. Compared with A-site sample, B-site substitution has higher defect density which could enhance ET probability of CR process, i.e. $^2H_{11/2} + ^4I_{15/2} \rightarrow ^4I_{9/2} + ^4I_{13/2}$. Then the Er^{3+} ions at $^4I_{13/2}$ state populate the $^4F_{9/2}$ state through ESA, which enhances the relative intensity of the red emission [8]. Furthermore, the population of $^4S_{3/2}$ state will decrease because a part of Er^{3+} ions populate the $^2H_{11/2}$ state [21], which also weakens the integrate intensity of the green emission. Therefore, the green-to-red ratio of B-site doped sample decreases relatively to that of A-site substitution.

4 Conclusions

1) Er^{3+} -doped BaTiO_3 nano-luminescent films were fabricated on LaNiO_3 substrate by sol-gel method. The films only have the diffraction peaks of BaTiO_3 and the peaks (200) shift for Er^{3+} doped A-site or B-site film,

which indicates that Er^{3+} ions are doped efficiently into different sites of BaTiO_3 host.

2) B-site doped film has a worse crystalline than A-site substitution, which should be attributed to the oxygen-deficient nonstoichiometry in B-site doped films.

3) Strong green UC emissions at 528 and 548 nm were obtained under the excitation of a 980 nm laser diode. The different UC photoluminescence properties were observed for Er^{3+} -doped samples with different lattice sites. A-site doped film has a stronger integrated intensity of green emissions and a weaker relative intensity of red emissions, which could be related to the better crystalline and the weaker CR process respectively.

Acknowledgements

The authors are grateful to Dr. J. H. HAO and Y. ZHANG (The Hong Kong Polytechnic University) for technical support and useful discussion during the photoluminescence measurements.

References

- [1] BLOCK B A, WESSELS B W. Photoluminescence properties of Er^{3+} -doped BaTiO_3 thin films [J]. Applied Physics Letters, 1994, 65(1): 25–27.
- [2] GILL D M, FORD G M, BLOCK B A, KIM S S, WESSELS B W, HO S T. Guided wave absorption and fluorescence in epitaxial $\text{Er}:\text{BaTiO}_3$ on MgO [J]. Thin Solid Films, 2000, 365(1): 126–128.
- [3] YANG Xu-dong, GUO Hai, CHEN Kun, ZHANG Wei-ping, LOU Li-ren, YIN Ming. Er^{3+} doped BaTiO_3 optical-waveguide thin films elaborated by sol-gel method [J]. Journal of Rare Earth, 2004, 22(1): 36–39. (in Chinese)
- [4] GILL D M, BLOCK A, CONRAD C W, WESSELS B W, HO S T. Thin film channel waveguides fabricated in metal-organic chemical vapor deposition grown BaTiO_3 on MgO [J]. Applied Physics Letters, 1996, 69(20): 2968–2970.
- [5] LIU Y X, PISARRDKI W A, ZENG S J, XU C F, YANG Q B. Tri-color upconversion luminescence of rare earth doped BaTiO_3 nanocrystals and lowered color separation [J]. Optics Express, 2009, 17(11): 9089–9098.
- [6] SCHLAGHECKEN G, GOTTMAN J, KREUTZ E W, POPRAW E R. Pulsed laser deposition of $\text{Er}:\text{BaTiO}_3$ for planar waveguides [J]. Applied Physics A, 2004, 79: 1255–1257.
- [7] POLMAN A. Erbium as a probe for everything? [J] Physica B, 2001, 300: 78–90.
- [8] ZHANG Y, HAO J H, MAK C L, WEI X H. Effects of site substitutions and concentration on Up-conversion luminescence of Er^{3+} -doped perovskite titanate [J]. Optics Express, 2011, 19(3): 1824–1829
- [9] ZHANG H X, KAM C H, ZHOU Y, BUDDHUDU S, XIANG Q, LAM Y L, CHAN Y C. Green up-conversion luminescence in $\text{Er}^{3+}:\text{BaTiO}_3$ films [J]. Applied Physics Letters, 2000, 77(5): 609–611.
- [10] DUNBAR T D, WARREN W L, TUTTLE B A, RANDALL C A, TSUR Y. Electro paramagnetic resonance investigations of lanthanide-doped barium titanate:dopant site occupancy [J]. Journal of Physics Chemistry B, 2004, 108(3): 908–917.
- [11] TAKSDA K, CHANG E, SMYTH D M. Rare-earth addition to

- BaTiO₃ [J]. *Advanced Ceramics*, 1987, 19: 147–152.
- [12] MITIC V V, NIKOLIC Z S, PAVLOVIC V B, PAUNOVIC V, MILJKOVIC M. Influence of rare-earth dopants on barium titanate ceramics microstructure and corresponding electrical properties [J]. *Journal of American Ceramics Society*, 2010, 93(1): 132–137.
- [13] WEN C H, CHU S Y, JUANG Y D, WEN C K. New phase transition of erbium-doped KNbO₃ polycrystalline [J]. *Journal of Crystal Growth*, 2005, 280(1–2): 179–184.
- [14] CHEN L, LIANG X L, LONG Z, WEI X H. Upconversion photoluminescence properties of Er³⁺-doped Ba_xSr_{1-x}TiO₃ powders with different phase structure [J]. *Journal of Alloys and Compounds*, 2012, 516: 49–52.
- [15] ZHANG H X, KAM C H, ZHOU Y, HAN X Q, XIANG Q, BUDDHUDU S, LAM Y L, CHAN Y C. Photoluminescence at 1.54 μm in sol-gel-derived, Er-doped BaTiO₃ films [J]. *Journal of Alloys Compounds*, 2000, 308: 134–138.
- [16] HUANG L M, CHEN Z Y, WILSON J D, BANERJEE S, ROBINSON R D, HERMAN I P, LAIBOWITZ R, BRIEN S O. Barium titanate nanocrystals and nanocrystal thin films: Synthesis, ferroelectricity and dielectric properties [J]. *Journal of Applied Physics*, 2006, 100: 034316.
- [17] JIANG C G, FANG L, SHEN M R, ZHENG F G, WU X L. Effects of Eu substituting positions and concentrations on luminescent, dielectric, and magnetic properties of SrTiO₃ ceramics [J]. *Applied Physics Letters*, 2009, 94: 071110.
- [18] GAO F, WU G H, ZHOU H, BAO D H. Strong up-conversion luminescence properties of Yb³⁺ and Er³⁺ co-doped Bi₄Ti₃O₁₂ ferroelectric thin films [J]. *Journal of Applied Physics*, 2009, 106:126104.
- [19] HAO J H, STUDENIKIN S A, COCIVERA M. Transient photoconductivity properties of tungsten oxide thin prepared by spray pyrolysis [J]. *Journal of Applied Physics*, 2001, 90(10): 5064–5069.
- [20] WANG Z L, CHAN H L W, LI H L, HAO J H. Highly efficient low-voltage cathodoluminescence of LaF₃:Ln³⁺ (Ln=Eu³⁺, Ce³⁺, Tb³⁺) spherical particles [J]. *Applied Physics Letters*, 2008, 93(14): 141106.
- [21] OKAMOTO E, SEKITA M, MASUI H. Energy transfer between Er³⁺ ions in LaF₃ [J]. *Physical Review B*, 1975, 11: 5103–5111.

Er³⁺掺杂位置对 Er³⁺:BaTiO₃ 薄膜上转换发光的影响

陈磊, 魏贤华, 傅旭

西南科技大学 四川省非金属复合与功能材料重点实验室—省部共建国家重点实验室培育基地, 绵阳 621010

摘要: 采用溶胶-凝胶法在 LaNiO₃/Si 衬底上制备 Er³⁺掺杂 BaTiO₃ 薄膜。通过 XRD、AFM 和 PL 图谱分别研究薄膜的晶体结构、形貌以及上转换发光性能。结果表明, 薄膜的微观结构和发光性能与 Er³⁺掺杂晶格的位置有关。A 位掺杂薄膜较 B 位掺杂薄膜具有较小的晶格常数和较好的结晶。PL 光谱表明: A 位掺杂的薄膜和 B 位掺杂的薄膜都于 528 nm 和 548 nm 处获得较强的绿色上转换发光以及在 673 nm 处获得较弱的红光, 分别对应 Er³⁺离子的 ²H_{11/2}→⁴I_{15/2}, ⁴S_{3/2}→⁴I_{15/2} 和 ⁴F_{9/2}→⁴I_{15/2} 能级跃迁。相对于 B 位掺杂的薄膜, A 位掺杂样品有较强的绿光发射积分强度以及较弱的红光发射相对强度。这种差异可以通过薄膜的结晶状况和交叉弛豫机制来进行解释。

关键词: Er³⁺掺杂; BaTiO₃ 薄膜; 上转换发光; 溶胶-凝胶法

(Edited by YANG Hua)